Adaptive Fuzzy Logic Control with PI Strategies for VSC Based HVDC Transmission Systems to Improve Black-Start Capability

1. Pentakota Jyothsna, M Tech Student, Dept of EEE,
DIET, Anakapalli, Andhra Pradesh.
Email: Jyothsnabojia@gmail.com
2. Jami Deleep Kumar,Associate Professor,Dept of EEE,
DIET, Anakapalli, Andhra Pradesh.
Email: Jdkumar@diet.edu.in

Abstract

The HVDC transmission system is a large power system. including those Economic growth, quicker recovery rate, frequency conversion, bulk power transmission, and quick sending and receiving controllability. These goals are not going to be simply or quickly accomplished with the HVAC system. This study takes into consideration the quicker recovery rate, while performing fault and maintenance, which is also known as the "black start" feature.This can be successfully accomplished when the real power is controlled at the receiving end controls DC link voltage. Superior sending and receiving control mechanisms are needed, rapid-acting phase-locked loops (PLL), and quicker controllers that are both intelligent and flexible play an essential role. As a result, novel PLL and fuzzy adaptive PI control techniques that are both quicker and more effective are being considered as possible solutions to the problem of the black start rate of HVDC lines. Both a classic PI controller using a conventional approach and a f adaptive fuzzy PI controller (FPIC) are utilized in this test to validate the performance of the proposed system. MATLAB and SIMULINK are the programs that are used to check the results.

Keywords: *HVDC system ; Black start, phase locked loop (PLL); advance Fuzzy adaptive PI controlle (FPIC)r; voltage source converte (VSC).*

DOINumber: 10.48047/nq.2022.20.11.NQ66844 **NeuroQuantology2022;20(11): 8501-8515**

1. Introduction

Energy demand is on the rise, and finding ways to meet it while also transporting energy from power plants to outlying locations is proving to be a difficult task. As a result of the high charging current and capacitance losses, AC transmission is difficult to employ for this purpose because of the lengthy distance required and the high charging current and capacitance losses. The key limitation preventing an AC link from connecting the unsynchronized grids to the existing grid is the voltage level and frequency. DC transmission can be used as a solution to the above challenge, where a controlled DC transmission allows for bulk power delivery over a long distance using a DC link.A controlled power flow is made possible by the use of converter stations at the generating end for AC/DC conversion. As a result of rapid advancements in power electronics switches, a better, more efficient control mechanism is available for power flow control.

There are two basic types of converter technology in HVDC transmission. [3] Classical CSCs and self-commutated voltage sourced converters (VSCs) are the two types. Line commutated current source converters with thyristor valves were the foundational technology for DC transmission in the 1950s for classical HVDC technology. In applications where thyristors are used to control power flow, their use is restricted because they are not fully controlled switches. IGBTs, which are fully controllable switches, are used in voltage source converter based transmission technology to provide one of the most efficient control mechanisms for controlling power flow in the transmission. Classical and VSC-HVDC are used for applications such as long distance transmission, underground and undersea cable transmission, and interconnection of asynchronous networks.. In terms of control,

VSC-HVDC is more flexible and efficient because it is able to control both active and reactive power independently of each other in order to maintain stable voltage and frequency. Using long-distance submarine cables and NIT RKL 3 VSC transmission technology's Self-commutation, system , dynamic voltage management, and black start can service isolated loads [6]. Classical high-voltage direct current (HVDC) is primarily used for long-distance point-to-point transmission of large amounts of power over land or sea cables. Due to the inability to turn off thyristors immediately, it has drawbacks like commutation failure and requires 40-60% of the total active power transmission as reactive power. There is no commutation problem, active and reactive power control is independent, no reactive power compensation is required, filter requirements are less as to filter out high frequency signals from PWM, no need for telecommunication between two stations of VSC-HVDC system [7]-[9]. IGBTs are used as a solution.

A similar DC link includes enormous DC capacitors and DC cables, plus two voltage sourced converters (VSCs).Two stations' active power can be coordinated by controlling the DC side voltage of a converter, while the active power is controlled by a different converter at the other station. A constant DC voltage source results in a "slack bus" that automatically controls power flow between stations. The AC voltage and reactive power controls can be switched as needed.

The HVDC technologies can be classed into two categories based on their terminal voltage and current waveforms at their DC side, the current source converter (CSC) and the voltage source converter (VSC). The CSC keeps the DC current at the same polarity and therefore the direction of the power flow through the converter is determined by the polarity of the DC voltage. These converters are built with semi controllable switches such as thyristors. Thyristors can only control the instant (ring angle) at which the current starts to conduct by a gate signal. However the current interruption is only determined by the zero crossing of the AC voltage. The DC side of a CSC is typically connected in series of large smoothing reactors that maintain the current continuity [5, 6]. The CSC generates voltage and current harmonics on the AC side. Large AC alters are needed to remove those types of harmonics. Today power ratings up to 10 000 MW with a DC voltage of 1 -100 kV and a transmission distance of more than 3 000 km are possible [7]. On the contrary, the VSC keeps the DC voltage at the same polarity and the direction of the power flow is determined by the polarity of the DC current. These converters are built with fully controllable switches such as IGBTs. These switches are able to conduct and interrupt the current at any instant by a gating command. The DC side of a VSC is typically connected in parallel with a relatively large capacitor that resembles a Voltage source [5]. In more recent converter designs, so called modular multilevel converter (MMC), the DC side capacitor is split into levels to reduce the AC harmonics [8, 9]. The VSC generates much less voltage and current harmonics on the AC side. Hence, only small alters are needed or with more recent converter design they could even be omitted. Because of this, the size of the converter stations is reduced dramatically. This opens up a new area to the HVDC technology like onshore converters or converter stations in urban areas. Nowadays VSC-HVDC links of up to 2 600 MW with a DC voltage of up to 525 kV and a transmission distance of more than 1 500 km are possible [10]. In Figure 1.1 a comparison of the deferent structure of a CSC and a VSC is shown. Table 1.1 gives a brief comparison of the two technologies. The Main deference between CSCs and VSCs is that the VSCs are able to Control the active and reactive power injections independent from each other as well as from the system state. This property makes VSC-HVDC links attractive for real-time power system control. They are also able to reverse power quicker than CSC-HVDC links, because they do not need to change the voltage polarity of the DC cable and thereby to discharge and charge the DC capacitor [12, 11]. Another advantage of VSCs is that they can be connected to weak AC networks. Theoretically, they are able to connect to an AC bus with a short-circuit ratio of 0, whereas CSCs need at least a short-circuit ratio of around 2 [13]. Voltage source converters are very important during a grid restoration. Since they do not need any short-circuit capacity in order to connect to the grid, they can start immediately and

provide voltage support [14]. Current source converters on the other hand can only start with sufficient short-circuit capacity.

2. Literature review

As modern society develops, so does its need for and reliance on power. Accidental blackouts have worsened. We should restore system power fast in case of emergency outages to avoid economic damages. Black-start technology is needed since large power outages are inevitable. A self-regenerating generator powers black start. This technique has been researched extensively. worked in domestic and worldwide power outages. As stated further, the approach has flaws. Under start power capacity, each unit's restoration sequence must be black-started. It also deals with black-start power supply setting in typical black start systems.System requirements for a successful black start include the following: Make sure you have enough black-start power to ensure that you have enough power for the initial startup. As a result ofMost loads are powered by asynchronous motors, which means they don't have enough power to start up.This leads to changes in the bus voltage and bus frequency. If this variation is greater than the permissible variation ofIf something happens to the motor, it will be unable to start. An adequate supply of electricity is essential to the operation of a business.The first eight races [1–8] were a success.There are currently three techniques for generating power in the event of a blackout.HVDC Voltage Source-Line Commutator Microgrids and HVDC (VSC-HVDC) Past applications have shown their potential.The LCC-HVDC system is operational when it is in use.An AC network is required to supply the commutation current for this device. Thus,When used as a black-start power supply, LCC-HVDC has some restrictions [17].Renewable energy sources are used to generate electricity in microgrids, which can start up on their own when the power goes out. However,It has a modest output and is restricted to a small area. Additionally, micro-grids have a lot to offer.if it is employed as a black-start power supply [18,19]. For example, compared to micro-gridsIn terms of start capacity, safety, and stability, VSC-HVDC is capable of meeting the needs of a wide range of applications. in terms of the initial carrying capacity. It is capable of independently controlling active and reactive power during a black start.with the potential to be integrated with the air conditioning system. Quick-response power can also be provided by this device and provide AC systems with voltage support [20–24]. VSC-HVDC increasingly uses MMC topologies. Modular Multilevel Converter-High Voltage Direct Current (MMC-HVDC). VSC-HVDC black-starting currently the subject of numerous investigations both at home and abroad.disaster-recovery power supply. The majority of the studies, on the other hand, focus on two- or three-level analyses.No research has been done on MMC-HVDC structure or VSC-HVDC topologies. As a result, we can VSC-black-start HVDC's capability cannot be applied in its entirety to aThe MMC-HVDC architecture. A black start power source is required for MMC-HVDC to function properly.in order to examine the MMC-HVDC converter. As a result, a thorough evaluation of the situation can be made.black-start performance of an MMC-HVDC power supply be made. The conventional black-and-white startA black start phase, grid restoration phase, and load restoration phase may be distinguished in the scheme.During the black start phase, the black-start power source is most active. The moment the power source goes black,grid and load restoration are carried out utilizing the non-black units that have been successfully started.Black start power supply and non-black starter devices. The primary purpose of a power source with a black start isThe black start scheme's initial stage is mirrored in this. This study mostly draws on previous researchblack start control techniques for MMC-HVDC, including pre-start control technique, the start-up no-load transmission line overvoltage suppression approach, and the start-up non-blackbegin the control plan for units. Complete power can be supplied via MMC-HVDC as a black-start power source.MMC-HVDC is being tested as a black-start power source with a network restoration method.source. Finally, PSCAD/EMTDC verifies the final black start scheme. The results of the simulationsthe system voltage and frequency are stable during black start, confirming the validity of the black start.Black-start electricity from MMC-HVDCFuzzy, sliding mode control, internal model

control, neural networks, and adaptive fuzzy PID controllers help synchronize HVDC terminals after blackstart [20]. [21] uses tiny signal analysis to study the impact of short circuit ratio and PLL in steady state. Mathematical modeling helps future study comprehend parameter efficacy and dependancy. So, sensitivity analysis helped understand normal and abnormal grid behavior and HVDC transmission consequences. Fast-acting and intelligent controllers are essential for speedy and effective system transitions. For faster and more adaptable responses, prior writers used ANFIS [22], Takagi-Sugeno fuzzy controller [23], and fuzzy logic-based adaptive droop control [24]. Adaptive fuzzy logic with PI controller is utilized in both sending and receiving end converters, coupled with PLL and control systems. Section 2 discusses HVDC black-start. Section 2 describes the adaptive fuzzy PI controller, while Section 4 describes the sending and receiving end control algorithms. Section 5 compares simulation results using conventional PI and traditional control schemes with our suggested adaptive fuzzy logic with PI controller. The 2030 EU Council climate and energy targets to use 45% RES for electricity generation are a major driver of the European power system change [1].

Massive implementation of RES could create bottlenecks that hinder network security and market integration. Transmission System Operators (TSO) in Europe are improving and modernizing their networks to unclog congested corridors and maintain power flow controllability. Permits, finance, and public approval could delay network reinforcement. The first two factors can be partially controlled through stakeholder engagement and a solid regulatory framework with energy transition-friendly rates. Third, neutralizing the environmental impact of an overhead power line is nearly impossible despite efforts. Underground AC transmission lines are unfavourable for long-distance power transmission. HVDC systems are popular because they meet environmental and technical requirements [2].Voltage Source Converter (VSC) technology enables versatility, dynamic voltage support, and active/reactive power controls [3].FIL will use 2x600MW VSC technology.HVDC can restore power to a blacked-out AC grid without short-circuiting. TSOs restore top-down and bottom-up [4].Other TSOs restore a TSO's system top-down. Bottom-up restoration re-energizes a TSO's system without other TSOs. Hydro production units can start without bus bar electricity in a typical restoration procedure. Traditional load recovery requires a TSO to control frequency and voltage to avoid system protections, generator or load disconnection, and component damage (e.g. caused by over-voltages). Inertia, frequency/voltage dynamic response, controller performance, etc. affect strategy efficacy. HVDC converter stations as restoration sources give power electronic control flexibility, but require proper management of decreased inertia restoration paths. VSC-HVDC systems utilise electro-static energy stored in capacitors and active networks to alter frequency during load pickup [5].

Due to HVDC's increased regulating energy, the restoration process can be sped up. Literature [15-18] discusses VSC-HVDC black start. This study validates an actual VSC HVDC control system in black start operation based on the frequency behavior mentioned above. This study uses the 2x1000 MW INELFE link (France-Spain HVDC interconnection) as an example [10].

3.Black-start HVDC transmission

Fig.1 shows a conventional HVDC transmission system. Area 1 AC power system includes generators, converter transformers, and ac filters. Right side power system contains generators and load stations powered by station 1. This is the RE station. Station 1's rectifier converts ac to dc and controls power, while station 2's inverter controls dc link voltages and current flow. This enhances restart rate, real and reactive power flow regulation, and fault ride through.

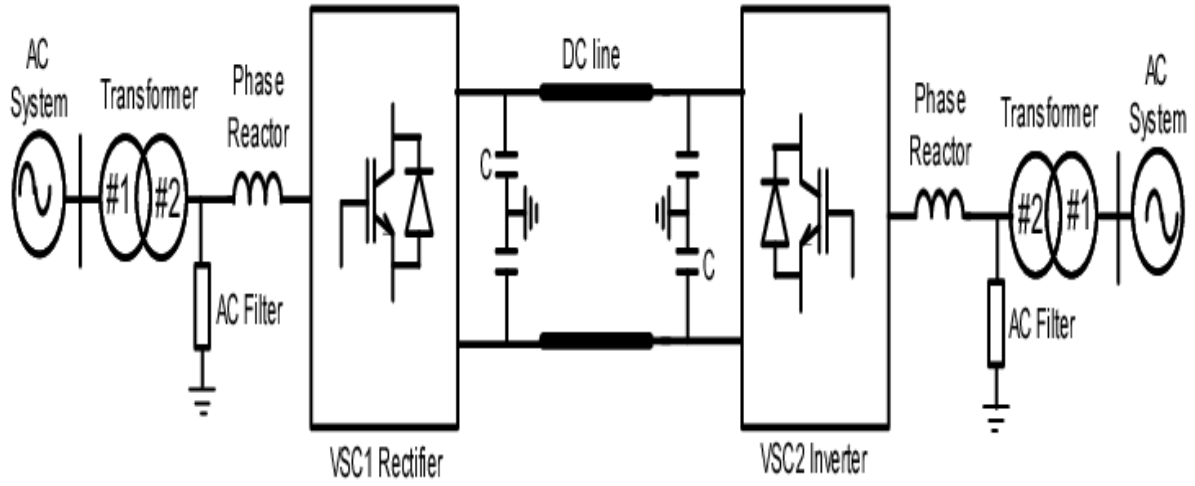

Fig.1. Two-area VSC- HVDC system.

Fig.2 shows MATLAB/ SIMULINK design and modelling of Fig.1 HVDC system .Generator stations with synchronous generators and stepup transformers are located on the left and right side blocks, respectively. The next set of blocks are the VI-measuring blocks and the RL parameters that represent the comparable transmission lines. Transformer and filters are displayed under Filter & Transformer block. VSI using IGBT and anti-parallel diode three-level neutral point clamped voltage source inverter is illustrated later. Nominal- blocks are used to depict the power cables that transmit the rectified power from station 1 to station 2. The dc long transmission system is shown here by an RL circuit. Reference is used to [16] for the system analysis.

In Fig.2, the HVDC converter link is depicted [16]. Vdc and Idc are the dc link voltage and current. The converter VSC switch receives Ii, which is the current flowing through the capacitor. Vcdq is a two-quadrant output voltage with an inverted potential. The current idq and voltage Vdq at the point of common coupling (PCC) of the LR inductive filter (smoking reactor) are proportional. The following is a breakdown of the mathematical analysis.

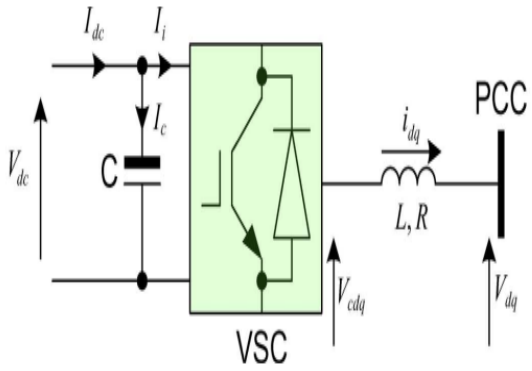

Fig.2 VSC-based HVDC system [16]

3.1 The setup of the dynamic current flow controller

This subsection derives the converter-to-PCC current as a transfer function to simplify system analysis. Fig.2 shows the dynamic dq axis ac current entering the PCC (1a and 1b)

$$\frac{di_d}{dt} = -\frac{R}{L} i_d + \frac{1}{L}(\psi_d) \quad (1a)$$

$$\frac{di_q}{dt} = -\frac{R}{L} i_q + \frac{1}{L}(\psi_q) \quad (1b)$$

Equations offer the d and q axis flux linkage for converter voltages and currents (2a and 2b)

$$\psi_d = V_{cd} - V_d + \omega_s L_s i_q \text{ (2a)}$$

$$\psi_d = V_{cd} - V_q + \omega_s L_s i_d \text{ (2b)}$$

Using equations (1a) to (2b), the dynamic dq axis ac current can be rewritten as in equations (3a and 3b)

$$\frac{di_d}{dt} = -\frac{R}{L} i_d + \frac{1}{L}(V_{cd} - V_d + \omega_s L_s i_q) \quad (3a)$$

eISSN 1303-5150

$$\frac{di_q}{dt} = -\frac{R}{L}i_q + \frac{1}{L}\left(V_{cd} - V_q + \omega_s L_s i_d\right) \text{(3b)}$$

The flux change to be controlled using a PI controller, it will work as current controller, so equations (2a and 2b) can be written in terms of PI controller proportional and integral coefficients like Kp and Ki as

$$\psi_d = K_p(i_d^* - i_d) + K_i\int(i_d^* - i_d)dt \quad \text{(4a)}$$

$$\psi_q = K_p(i_q^* - i_q) + K_i\int(i_q^* - i_q)dt \text{ (4b)}$$

For simplicity if dynamic angular d and q axis parameters and steady angular d and q axis are represented as shown in equations (5a and 5b) as

$$\dot{\omega}_d = \int(i_d^* - i_d)dt \text{ And } \dot{\omega}_q = \int(i_q^* - i_q)dt \text{ ,(5a)}$$

Then

$$\omega_d = (i_d^* - i_d) \text{ And } \omega_q = (i_q^* - i_q), \quad \text{(5b)}$$

Now, the dynamic current equations are further modified in terms of K_p and K_i coefficient as in (6a and 6b)

$$\frac{di_d}{dt} = -\frac{(R+K_p)}{L}i_d + \frac{1}{L}\omega_d + \frac{K_p}{L}i_d^* \quad \text{6a)}$$

$$\frac{di_q}{dt} = -\frac{(R+K_p)}{L}i_q + \frac{1}{L}\omega_q + \frac{K_p}{L}i_q^* \text{(6b)}$$

The dynamic angular speeds can also be written as

$$\frac{d\omega_d}{dt} = -\frac{K_i}{L}i_d + K_i i_d^* \quad \text{(7a)}$$

$$\frac{d\omega_q}{dt} = -\frac{K_i}{L}i_q + K_i i_q^* \quad \text{(7b)}$$

From the equations 6a to 7b, the dynamic currents depend on K_p parameters and angular speed depends on K_i parameters. Further rewriting the equations 2a and 2b, the reference d and q axis converter voltages will be of the form

$$V_{cd}^* = \psi_d + V_d - \omega L i_q \quad \text{(8a)}$$

$$V_{cq}^* = \psi_q + V_q + \omega L i_d \quad \text{(8b)}$$

Now manipulating and rewring the (6a) and (6b), the transfer functtion of d and q axis current will become as shown in the equation (9)

$$\frac{i_d(s)}{i_d^*(s)} = \frac{i_q(s)}{i_q^*(s)} = \frac{\frac{K_p}{L}s + \frac{K_i}{L}}{s^2 + \frac{(R+K_p)}{L} + \frac{K_i}{L}} \quad \text{(9)}$$

3.2 The dc link voltage and parameter dependency

The dc link voltage can be written using the Fig.2 as

$$c\frac{dV_{dc}}{dt} = I_{dc} - I_i \quad \text{(10)}$$

The inverter current Ii is written as a function of converter and dc link voltage and currents as

$$I_i = \frac{V_{cd}i_d + V_{cq}i_q}{V_{dc}} \quad \text{(11)}$$

So, using equations (10 and 11), the dc link voltage will be as in (12)

$$c\frac{dV_{dc}}{dt} = I_{dc} - \frac{V_{cd}i_d + V_{cq}i_q}{V_{dc}} \quad \text{(12)}$$

Now linearizing the equation (12) using Taylor series and neglecting the higher order terms and rewriting in the simpler and standard form as in eqation (13)

$$\frac{d\Delta V_{dc}}{dt} = \frac{\Delta I_{dc}}{C} + \frac{(V_{cd}i_d + V_{cq}i_q)}{CV_{dc}^2} - \frac{i_d}{CV_{dc}}\Delta V_{cd} - \frac{i_q}{CV_{dc}}\Delta V_{cq} - \frac{V_{cd}}{CV_{dc}}\Delta i_d - \frac{V_{cq}}{CV_{dc}}\Delta i_q$$

(13)

Further simplifying the equation (13), the (14) equation represents the change in dc link as

$$\Delta V_{dc} = \Delta i_{dc} - \frac{V_{cd}}{V_{dc}}\Delta i_d - \frac{V_{cq}}{V_{dc}}\Delta i_q - \frac{i_d}{V_{dc}}\Delta V_{cd} - \frac{i_q}{V_{dc}}\Delta V_{cq}$$

(14)

Choosing PI controller coefficients Kp and Ki based on HVDC link black start is crucial. PI controller effectiveness depends on proper tuning and system response. Quicker controllers can provide speedy and accurate control. Also, choosing the right dc link voltage to maintain it practically constant with variations in ac voltage and current is crucial.

4. Proposed Fuzzy adaptive PI controller (FPIC)

Figure 3 provides a schematic representation of the Fuzzy-PI controller. The reference is taken from the work [25], which provides an overview of the controller's design as well as its fundamental explanation. For efficient command and control of the HVDC system, the same controller [6] was identified. Fuzziness adaptive PI controller for black start of HVDC has been designed as part of this

eISSN 1303-5150

body of work. The purpose of this design accelerates launch. reaction while also ensuring that the functioning is as smooth a possible.The outer loop limits voltage, the inner loop limits current.

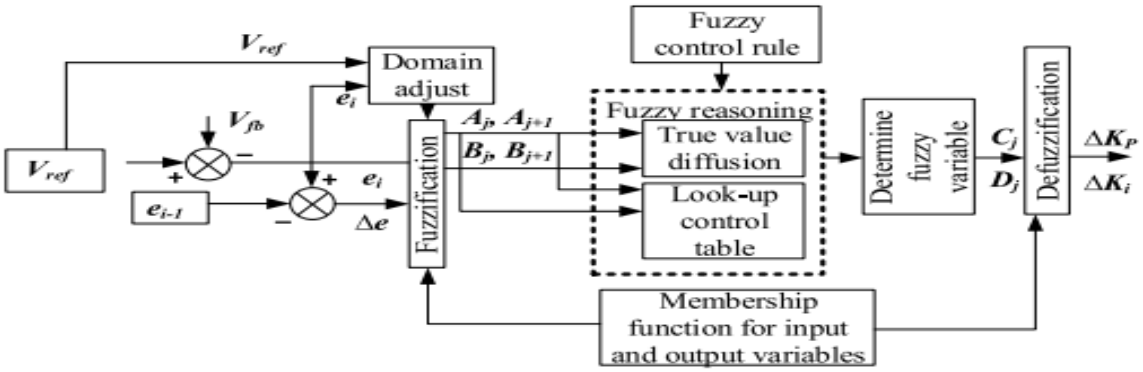

Figure 3: Conventional Adaptive Fuzzy- PI Control (FPIC) [25].

For this, the PI coefficient parameters Kp and Ki are the inputs, and the change in PI coefficient parameters Ki are the outputs. The fuzzy adaptive controller uses the input error as its primary reference. A voltage error or current error may be present, depending on the control action that is taken. The voltage will be The outer loop limits voltage, the inner loop limits current. In general, the internal controller is more responsive than the external controller. Consequently, the inner loops are crucial and A more robust design is needed for good response time and steady values. Are to be attained. Fuzzy set is given the error parameter, which is broken down into proportional and derivative errors. Now, the fuzzifier will use the lookup table scheme and the adopted rules to generate some membership values. The defuzzifier block then takes these membership signals and turns them into conventional signals with two output points, Kp and Ki. However, these numbers can fluctuate depending on Mamdani fuzzy se's membership and rules even if the error value remains constant.t.

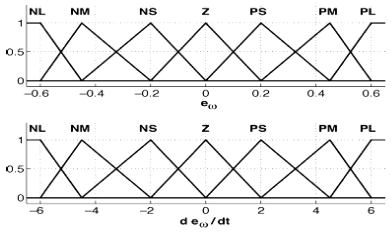

Fig. 4. Fuzzy logic membership functions.

TABLE I
FUZZY LOGIC RULES

$\dot{e}_w$ \ e_w	NL	NM	NS	Z	PS	PM	PL
PL	Z	PL	PL	PL	PL	PL	PL
PM	NS	Z	PS	PS	PL	PL	PL
PS	NL	NS	Z	PS	PS	PL	PL
Z	NL	NL	NS	Z	PS	PL	PL
NS	NL	NL	NS	NS	Z	PS	PL
NM	NL	NL	NL	NS	NS	Z	PS
NL	NL	NL	NL	NL	NL	PL	Z

Figure 4. Fuzzy Logic Membership function

Figure 4 depicts the error in Faulty feedback rate and probabilistic reasoning membership. Table 1 shows the rules for defuzzification. The Margin of error given by the vertical columns, while the error parameters are given by the horizontal parameters. It is the relationship between the two of these that determines the defuzzification method. There are no mathematical representations for the fuzzy memberships and rules, but they are simple to build. As a result, Fuzzy controllers are easy to design and implement and offer faster control

eISSN 1303-5150

action and fast transient and transitory response. An abstracted generalized conception of the fuzzy adaptive PI controller's design is depicted in Figure 5. layers 2 and 3 are intermediary layers that process the input parameters x1, x2,... xn. They are referred to as W11, W12, W21, and Wm respectively, W11, W12, Wrm.There are y1, y2,..., ym for each output. t these have n inputs, r reaction products, and m outputs. He usual form, as shown in Fig. 5. Fuzzy performance relies heavily on the weight modifications in layers 2 and 3.

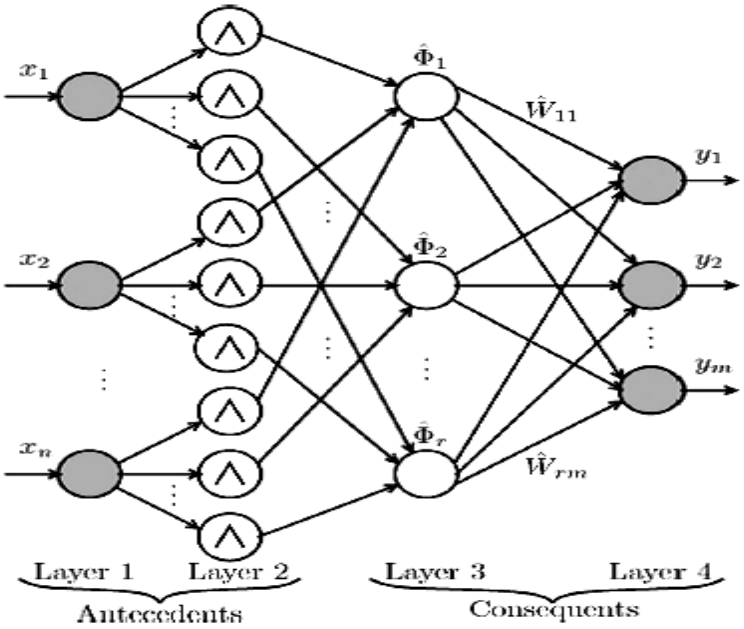

Fig. 5. Adaptive fuzzy logic control structure.

Figure 6 depicts the Fuzzy-PI controller created using the MATLAB/SIMULINK package in action. Here, we're dealing with errors (e) and the rate at which those errors change (edot). The MAMDANI-based model is used to create the fuzzy adaptive PI. The three outputs are the KPP and Kdp proportional and integral parameters, as well as the alpha value. Figure 7 depicts the surface PI fuzzy controller diagram.

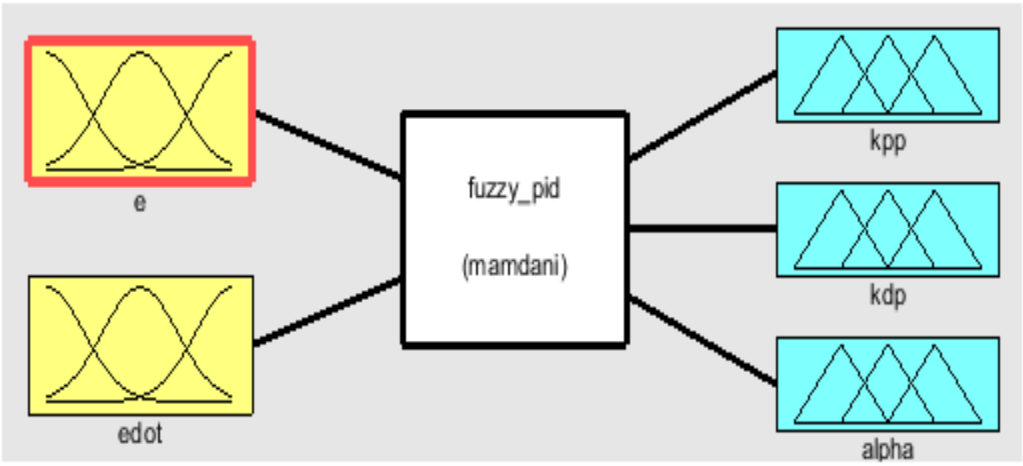

Fig.6 MATLAB/Simulink public library: Adaptive fuzzy-adaptive PI controller (FPIC)

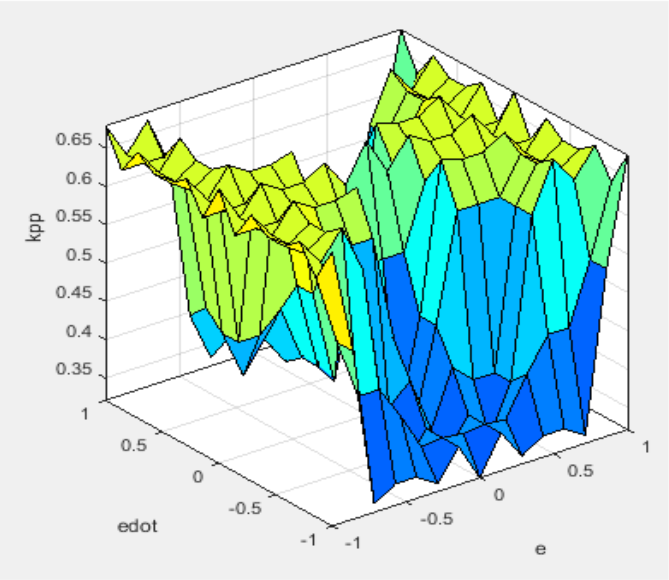

Fig.7 Adaptive fuzzy-adaptive PI controller (FPIC) surface diagram

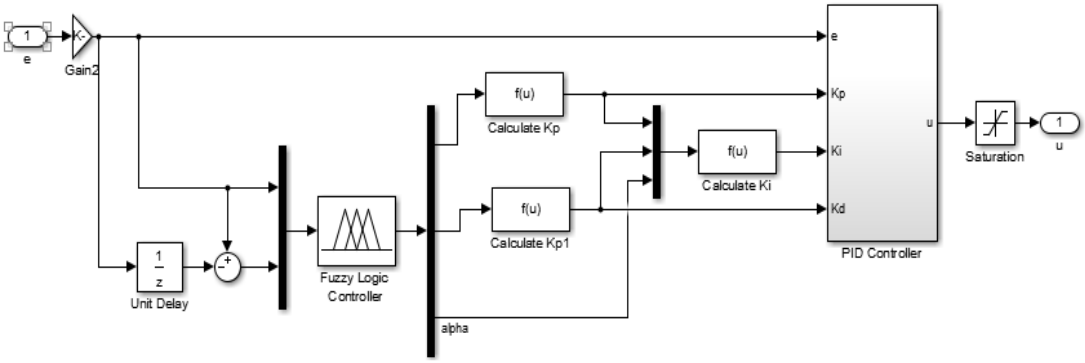

Fig.8a. Adaptive fuzzy-adaptive PI controller (FPIC) MATLAB/SIMULINK design

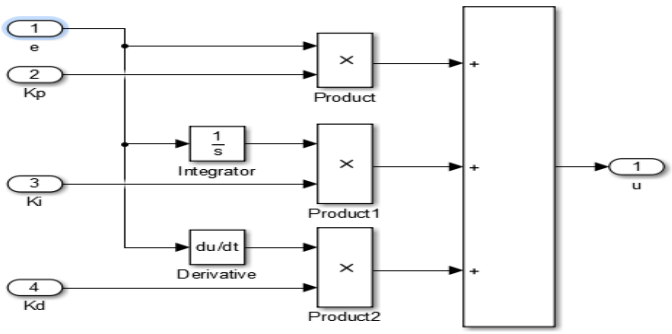

Fig.8b. MATLAB/SIMULINK model of Adaptive fuzzy-adaptive PI controller (FPIC)

Figure 8a illustrates the fuzzy-adaptive PI controller MATLAB/Simulink model and Figure 8b the intrinsic PID controller. This model has zero speculation. For 1 & 2 controller, the Kp calculation has been

eISSN 1303-5150

provided below. if you want to know how much u is in a kp1 calculation, you need to know how much u is in a kpp1 calculation.The equation that follows describes the integral coefficient parameter in detail. (u(1)2/(u(2)*u(3))), which is the Ki formula.

Figure 9a depicts Figure 9a shows the inverter station converter scheme, and Fig. 9b shows the inverter authority. Bus voltage, line currents, and existing to the rectifier and inverter provide bus voltage and line currents. Per-unit (p.u.) values are used for all of the parameters. Using the phase locked loop, you may synchronize your system and retrieve information such as the phase sequence and frequency characteristics. Fuzzy-adaptive PI controllers replace the traditional PI controllers in this design..

4.3.The control schemes for rectifier and inverter stations

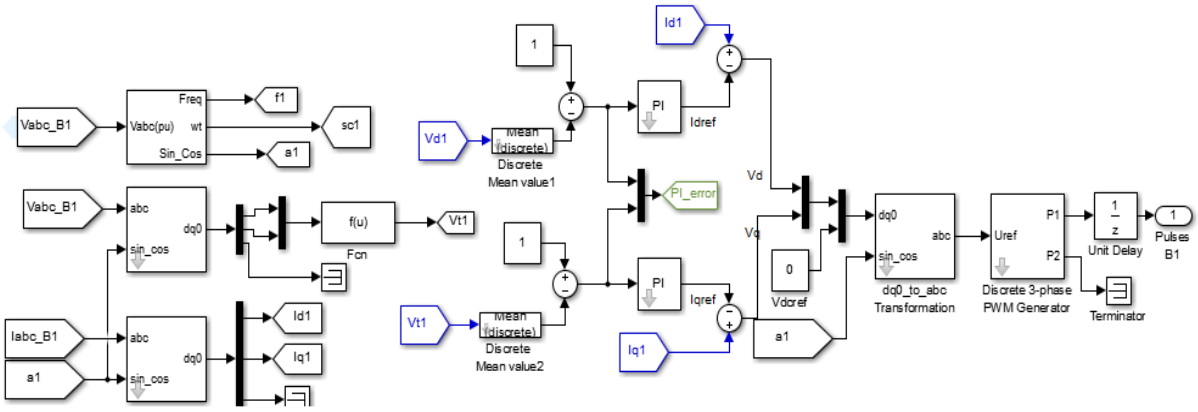

Fig.9 Controller design for HVDC black-start

5.Result Analysis

5.1 Vsc-Hvdc Perfomance Result and Discussion

Fig. 10a from [19] shows the paper's HVDC transmission line test system. System has two areas with two AC power plants each. The distance is represented as RL parameters, the venin equivalent. Observe the AC sensor station. The left-side rectifier 1 and the right-side inverter 2 convert AC to DC. Stepup converters power the 11-bus system. VSC1 and VSC2 are IGBT-switching rectifier and inverter stations. Fig. 10b shows a MATLAB/Simulation-based two-area HVDC transmission system with optimized blackstart capability.

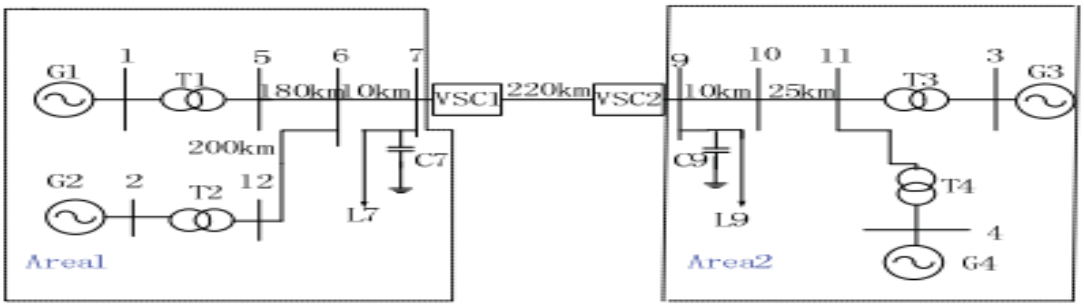

Fig.10a Dual HVDC station test system considered for the black-start of HVDC [19]

eISSN 1303-5150

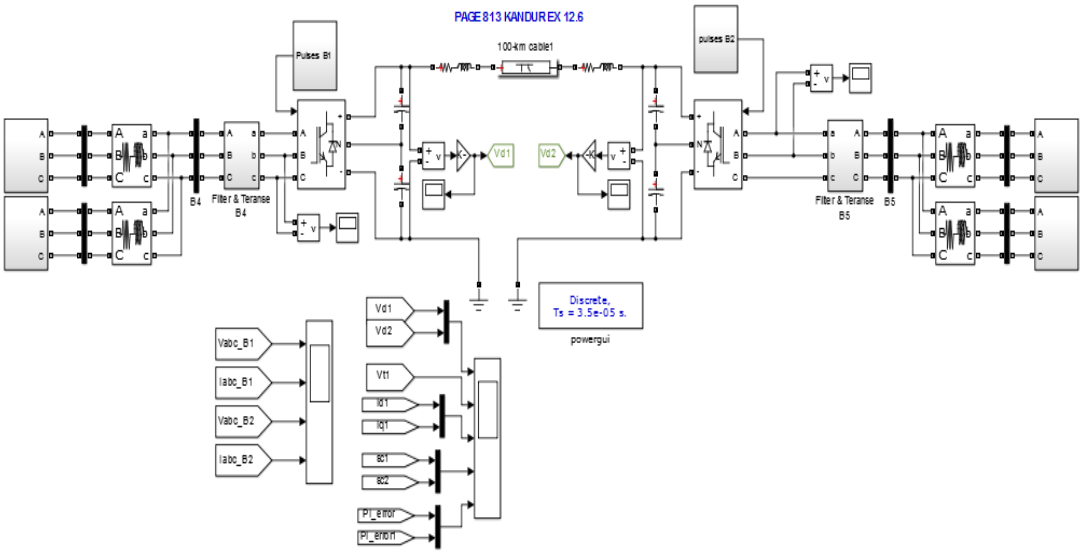

Fig.10b MATLAB/SIMULINK-based two-area HVDC transmission for better blackstart

Utilizing the PI controller and the fuzzy-adaptive PI Figures 11 and 12 demonstrate HVDC black-start regulator outputs with MATLAB/SIMULINK. Respectivel.When the system is restarted after being maintained or repaired; there is either no current or none 05 seconds at the station. The bus 1 and 2 voltage levels at the rectifier and inverter ends of Fig. 1a are constant and at 1.0 p.u. This is demonstrated by the figures shown in Fig. 11 (ii).There was an increase in the current flowing through these buses when the system was restarted at black-start using the con when the circuit was black-started in 0.05 seconds. Troller at 0.05 s. This increase in current gradually decreased until it reached The PI controller is steady after two cycles. On the other hand, if you use a fuzzy-adaptive PI controller, there won't be any surges, and as a result, neither the sub-transient nor the transitory characteristics of the waveform will be present (see Figure 11). (ii). the system started up quickly and did not experience any overshoots. In comparison to the performance of a conventional PI controller, the system's b Stable and effective behavior these qualities appear to be superior to those [15, 17, 18, 19] in the relevant body of scholarly research. Figures 11 (i) and 11 shows a comparison between the PI controller and the fuzzy-adaptive PI controller, which facilitates an easy analysis (b). Starting currents are approximately two times higher with a PI controller when using the conventional technique [17–19]. However, this value is only increased by 1.5 times when using a PI controller, and it is only increased by 1.01 times when using Fuzzy-PI controller. When used with the controller, the proposed method improved performance. I was observed when the fuzzy-adaptive PI controller was used.

eISSN 1303-5150

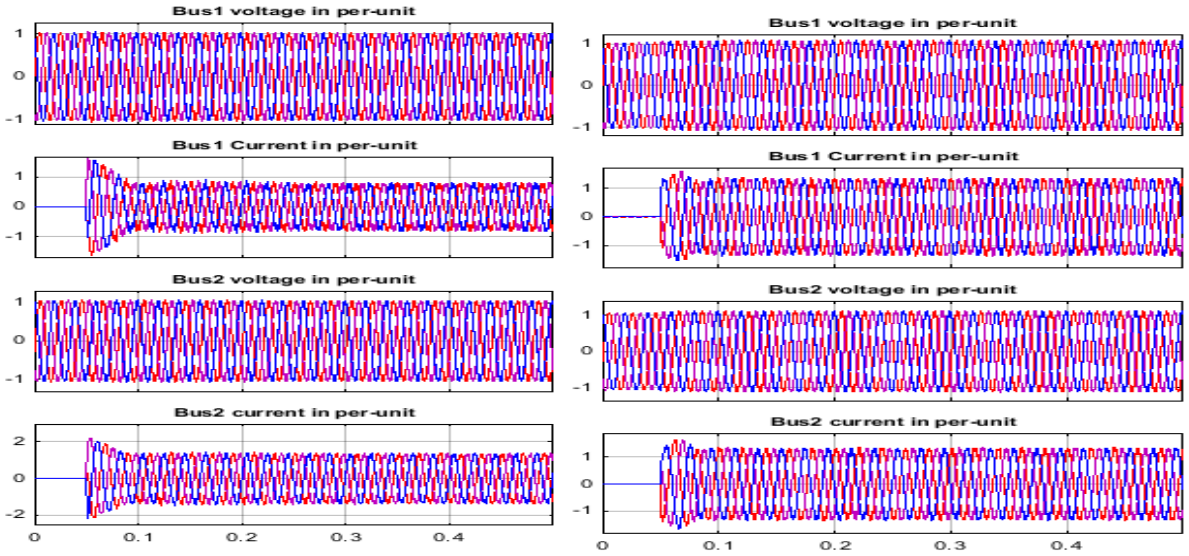

Fig.11 black-start VSC-HVDC bus voltages PI and fuzzy-adaptive PI controllers

Fig.12 I and (ii) compare PLL waveforms, PI and fuzzy adaptive controller output (error input dependency) (ii). From 0 to 0.05s, the DC link voltage is 1 Pu. Has been observed with a PI controller. The dc link voltage surges at 0.05 and settles at 0.2s when HVDC is launched as a black start. The fuzzy adaptive PI controller immediately stabilized the dc link voltage, which had been stable at 1pu until 0.05s, to a constant 1.03pu value.

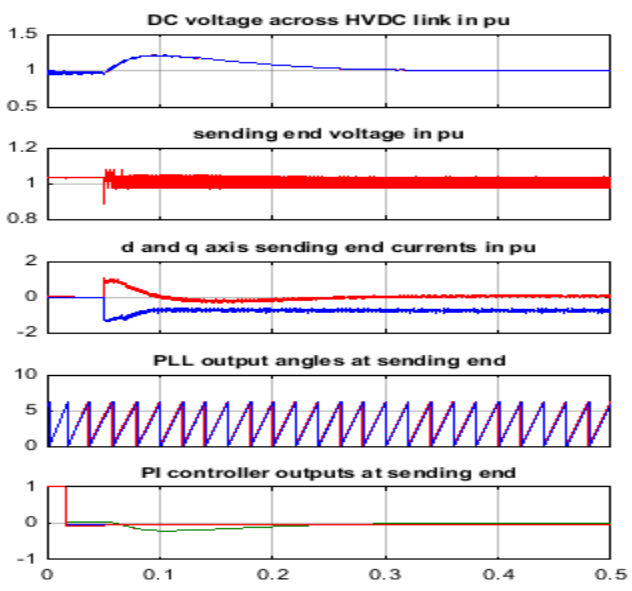

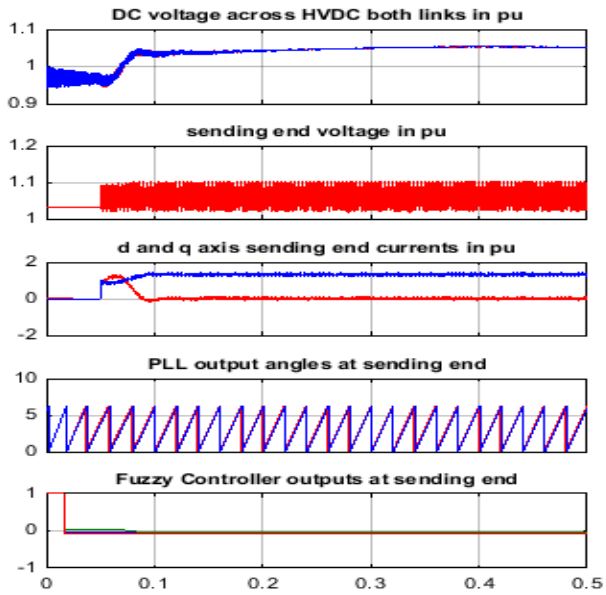

Fig. 12(1) PI controller scheme **Fig.12 (ii) fuzzy-adaptive PI scheme**

Fig.12 black-start VSC-HVDC bus voltages PI and fuzzy-adaptive PI controllers

There are no ripples in the sending end voltage magnitude when Fuzzy PI and PI controllers are used to turn off the HVDC station. There is, however, a notable change in voltage magnitude between the PI and the fuzzy adaptive PI controllers. The average value of the ripples is nearly identical for both controllers. Bus 6 receives an end current from the DQ-axis, regardless of whether it is PI or fuzzy adaptive PI. With the fuzzy adaptive PI controller, the d-axis current reached

eISSN 1303-5150

zero more quickly than with a conventional PI controller. After starting at zero current value, with the PI controller, there was an initial surge in the magnitude of the q-axis current before it slowly decreased and reached steady-state value; with fuzzy adaptive PPI controller, the magnitude of the q-axis current is maintained constant throughout. Both controllers appear to have the same PLL waveform. It is possible to see small deviations from zero value when looking at waveforms generated by PI controller and fuzzy adaptive PI controller, but no such deviations can be seen when looking at waveforms generated by the latter.

Hence, from the above analysis, it can be observed that the system behaviour is improved effectively with fuzzy adaptive PI controller than with PI controller. The quick the above analysis shows that the based logic PI controller improves control flow over the PI controller. Fuzzy control PI performs quickly and steadily. And steady performance is observed more with fuzzy adaptive PI con

Conclusion

This study this paper discusses the efficiency of a HVDC system using a fuzzy-based PI controller. When operating under black-start conditions. The rapid response, when begun from zero value, to reach a constant current value without surges and ripples is what is noticed for the purpose of the analysis. The purpose of this study is to design a brand new control system as well as an improved fuzzy adaptive PI controller. When compared with the traditional method, the system response time with the proposed method using PI controller is significantly shorter and does not include any transients. When using the identical PI controller, the starting currents at both ends of the converter are approximately twice as high as the works that are found in the body of scholarly research. Using the proposed control strategy with a PI controller results in a starting current value that is 1.5 times higher during a black start. Using a fuzzy-adaptive PI controller, however, reduces this value to 1.01 times, which is trivial at best. As a result, improved performance was shown when the proposed technique was used PI controller improved performance. was seen when the fuzzy-adaptive PI controller was used. The control technique is straightforward, dependent on fewer parameters, characterized by rapid response times, and reliable performance in operation.

References

[1] Felix, Busemann. "Direct current electric transmission system." U.S. Patent 2,684,461, issued July 20, 1954.

[2] Sarma, Maruvada P., and WasylJanischewskyj. "Corona loss characteristics of practical HVDC transmission lines, part I: unipolar lines." *IEEE Transactions on Power Apparatus and Systems* 5 (1970): 860-867.

[3] Rudervall, Roberto, J. P. Charpentier, and Raghuveer Sharma. "High voltage direct current (HVDC) transmission systems technology review paper." *Energy week* 2000 (2000): 1-19.

[4] Allebrod, Silke, Roman Hamerski, and Rainer Marquardt. "New transformer less, scalable modular multilevel converters for HVDC-transmission." In *2008 IEEE Power Electronics Specialists Conference*, pp. 174-179. IEEE, 2008.

[5] Johnson, Brian. "New Trends for HVdc: An Evolution of Applications Since 2007 [Guest Editorial]." *IEEE Power and Energy Magazine* 17, no. 3 (2019): 20-114.

[6] Hannan, M. A., I. Hussin, Pin Jern Ker, Md MurshadulHoque, MS Hossain Lipu, Aini Hussain, MS Abd Rahman, C. W. M. Faizal, and FredeBlaabjerg. "Advanced control strategies of VSC based HVDC transmission system: Issues and potential recommendations." *IEEE Access* 6 (2018): 78352-78369.

[7] Gao, Shuping, Hangiian Zhu, Baohui Zhang, and Guobing Song. "Modeling and simulation analysis of Hybrid Bipolar HVDC system based on LCC-HVDC and VSC-HVDC." In *2018 IEEE 3rd Advanced Information Technology, Electronic*

and Automation Control Conference (IAEAC), pp. 1448-1452. IEEE, 2018.

[8] Khazaei, Javad, Peter Idowu, ArashAsrari, A. B. Shafaye, and LakshanPiyasinghe. "Review of HVDC control in weak AC grids." *Electric Power Systems Research* 162 (2018): 194-206.

[9] Wu, Haitao, Yonghe Liu, Zhihe Wang, Lei Song, and Fan Wu. "Flexible CSC-HVDC system." *The Journal of Engineering*2019, no. 16 (2019): 2337-2342.

[10] Tada, Kimiko, Takamasa Sato, Atsushi Umemura, Rion Takahashi, Junji Tamura, Yoshiharu Matsumura, Daisuke Yamaguchi, Hirooki Kudo, Masakazu Niiyama, and YasuhitoTaki. "Frequency control of power system including PV and wind farms by using output frequency band control of HVDC interconnection line." *The Journal of Engineering* 2019, no. 18 (2019): 4879-4883.

[11] Sun, Jian, Mingjie Li, Zhigang Zhang, Tao Xu, Jingbo He, Haijiao Wang, and Guanghui Li. "Renewable energy transmission by HVDC across the continent: system challenges and opportunities." *CSEE Journal of Power and Energy Systems* 3, no. 4 (2017): 353-364.

[12] Farsani, PooyanMoradi, Nilanjan Ray Chaudhuri, and RajatMajumder. "Hybrid simulation platform for VSC-HVDC-assisted large-scale system restoration studies." In *2016 IEEE Power & Energy Society Innovative Smart Grid Technologies Conference (ISGT)*, pp. 1-5. IEEE, 2016.

[13] Benasla, Mokhtar, TayebAllaoui, MostefaBrahami, MouloudDenai, and Vijay K. Sood. "HVDC links between North Africa and Europe: Impacts and benefits on the dynamic performance of the European system." *Renewable and Sustainable Energy Reviews* 82 (2018): 3981-3991.

[14] Farsani, PooyanMoradi, Sai Gopal Vennelaganti, and Nilanjan Ray Chaudhuri. "Synchrophasor-enabled power grid restoration with DFIG-based wind farms and VSC-HVDC transmission system." *IET Generation, Transmission & Distribution* 12, no. 6 (2017): 1339-1345.

[15] Bahrman, Michael, and Per-Erik Bjorklund. "The new black start: system restoration with help from voltage-sourced converters." *IEEE Power and Energy Magazine* 12, no. 1 (2013): 44-53.

[16] Adam, Grain Philip, Khaled H. Ahmed, Stephen J. Finney, Keith Bell, and Barry W. Williams. "New breed of network fault-tolerant voltage-source-converter HVDC transmission system." *IEEE Transactions on Power Systems* 28, no. 1 (2012): 335-346.

[17] Wang, ChaoLiang, WenTao Lv, Yi Lu, Feng Xu, and Peng Qiu. "Start-up scheme for converter station of MMC-HVDC based on single-clamp sub-module using in grid black start." *The Journal of Engineering* 2019, no. 16 (2019): 1892-1896.

[18] Xia, Chengjun, Chengxiang Li, HaiwenLan, Zhaobin Du, and Yiping Chen. "Frequency regulation strategy based on variable-parameter frequency limit control during black start."*IET Generation, Transmission & Distribution* 12, no. 17 (2018): 4002-4008.

[19] Zhou, Mingxia, Sheng Li, Jianhua Zhang, Zongqi Liu, and Yinhui Li. "A study on the black start capability of VSC-HVDC using soft-starting mode." In *2009 IEEE 6th International Power Electronics and Motion Control Conference*, pp. 910-914. IEEE, 2009.

[20] Hannan, M. A., I. Hussin, Pin Jern Ker, Md MurshadulHoque, MS Hossain Lipu, Aini Hussain, MS Abd Rahman, C. W. M. Faizal, and FredeBlaabjerg. "Advanced control strategies of VSC based HVDC transmission system: Issues and potential recommendations." *IEEE Access* 6 (2018): 78352-78369.

[21] Zhou, Jenny Z., Hui Ding, Shengtao Fan, Yi Zhang, and Aniruddha M. Gole. "Impact of Short-Circuit Ratio and Phase-Locked-Loop Parameters on the Small-Signal Behavior of a VSC-HVDC Converter." *IEEE Transactions on Power Delivery* 29, no. 5 (2014): 2287-2296.

[22] Yang, Tian, and Ran Li. "Study on A Novel ANFIS Controller for VSC-HVDC." In *2015 International Industrial Informatics and*

Computer Engineering Conference. Atlantis Press, 2015.

[23] Nayak, Niranjan, SangramKeshariRoutray, and Pravat Kumar Rout. "Design of Takagi-Sugeno fuzzy controller for VSC-HVDC parallel AC transmission system using differential evolution algorithm." *International Journal of Computer Aided Engineering and Technology* 8, no. 3 (2016): 277-294.

[24] Chen, Xia, Long Wang, Haishun Sun, and Yin Chen. "Fuzzy logic based adaptive droop control in multiterminal HVDC for wind power integration." *IEEE Transactions on Energy Conversion* 32, no. 3 (2017): 1200-1208.

[25] H. Liang, G. Li, M. Zhou, and C. Zhao, ‘‘The implementation of fuzzy adaptive PI controller in VSC-HVDC systems,’’ in *Proc. IEEE/PES Power Syst. Conf. Expo.*, Mar. 2009, pp. 1–5.

[26] L. Li, M. Zhou, S. Li, Y. Li, “A New Method of Black Start Based on VSC-HVDC”, International Conference on Computing, Control and Industrial Engineering, 5-6 June 2010, Wuhan, China.

[27] B. Fend, X. Zhai, Y. Li, Z. Wang, “Experimental study on black-start capability of VSC-HVDC for passive networks” - IEEE PES Asia- Pacific Power and Energy Engineering Conference (APPEEC), 25-28 Oct. 2016, Xi'an, Chin.

[28] D. Cirio, E. Ciapessoni, A. Pitto, G. Giannuzzi, R. Zaottini “Support of VSC-HVDC to the restoration of weakly connected systems: the Sardinia case.”, CIGRÉ Paris Conference, 2018.

[29] P. Rault, F. Colas, X. Guillaud and S. Nguefeu, "Method for small signal stability analysis of VSC-MTDC grids," 2012 IEEE Power and Energy Society General Meeting, San Diego, CA, 2012, pp. 1-7.

[30] T. Midtsund, A. Becker, J. Karlsson, K. A. Egeland, “A Live Black- start Capability test of a Voltage Source HVDC Converter”, CIGRÉ Canada Conference, 2015.

eISSN 1303-5150